

# Supporting Information for “Reaction Mechanisms in Talc under Ionizing Radiation: Evidence of a High Stability of H<sup>•</sup> Atoms”

*Maxime Lainé,<sup>a</sup> Thierry Allard,<sup>b</sup> Etienne Balan,<sup>b</sup> François Martin,<sup>c</sup> H. Jurgen Von*

*Bardeleben,<sup>d</sup> Jean-Louis Robert,<sup>b</sup> Sophie Le Caër<sup>a\*</sup>*

---

<sup>a.</sup> LIONS, NIMBE, CEA, CNRS, Université Paris-Saclay, CEA Saclay, F-91191 Gif-sur-Yvette Cedex, France.

<sup>b.</sup> IMPMC, Sorbonne Universities, UPMC, CNRS UMR-7590, MNHN, IRD, 4 Place Jussieu, F-75252 Paris Cedex 05, France.

<sup>c.</sup> GET UMR-5563 CNRS-UPS-IRD-CNES, 14 Avenue Edouard Belin, F-31400 Toulouse, France.

<sup>d.</sup> INSP, Sorbonne Universities, UPMC, CNRS UMR-7588, 4 Place Jussieu, F-75252 Paris Cedex 05, France.

## Corresponding author:

Sophie Le Caër

e-mail: [sophie.le-caer@cea.fr](mailto:sophie.le-caer@cea.fr)

Phone: +33 1 69 08 15 58

## SI-1: Infrared spectroscopy of talc

Infrared (IR) spectra are recorded in transmission mode in the 4000-370  $\text{cm}^{-1}$  energy range with a Bruker Tensor 27 FT-IR spectrophotometer. 1% of sample is pelletized in KBr. All the spectra are collected with a 4  $\text{cm}^{-1}$  resolution from 100 scans. The data are analysed using the OPUS software. The background is obtained by measuring the spectrum of a pure KBr pellet and subtracted in all cases.

The infrared bands are identified by comparison with literature data.<sup>1-6</sup> The different vibrational modes together with their assignments are given in Table S1.

Wavenumber ( $\text{cm}^{-1}$ )	Vibrational mode
3677	isolated MgO-H stretching
1000-1200	Si-O-Si assymetric stretching
805	Si-O-Si symmetric stretching
530-700	Mg-OH stretching
420-470	Si-O-Si bending

**Table S1.** IR bands (position, assignment) detected in talc.

Figure S1 presents the IR spectrum of synthetic and natural talc. In the case of talc, only structural hydroxyl groups are present. No water molecules are detected in the sample, in agreement with TGA measurements.

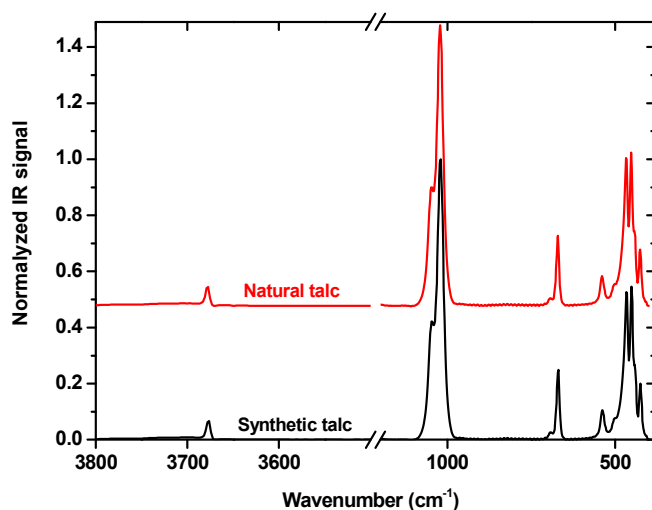


**Figure S1.** IR spectrum of synthetic talc (—) and natural talc (—) measured by transmission. Vibrational bands of water are not detected. The band at 2350  $\text{cm}^{-1}$  corresponds to  $\text{CO}_2$  present in the atmosphere of the spectrometer. Both synthetic and natural talc have the same IR spectrum. The spectrum of natural talc has been shifted for convenience.

## References:

- (1) Bertie, J.E., Ahmed, M.K. and Eysel, H.H., Infrared Intensities of Liquids. 5. Optical and Dielectric Constants, Integrated Intensities, and Dipole Moment Derivatives of Water and Water-D<sub>2</sub> at 22°C, *J. Phys. Chem*, **1989**, 93, 2210-2218.
- (2) Bishop, J.L., Pieters, C.M. and Edwards, J.O., Infrared Spectroscopic Analyses on the Nature of Water in Montmorillonite. *Clays Clay Miner.*, **1994**, 42, 702-716.
- (3) Robert, J.L. and Kodama, H., Generalization of the correlations Between Hydroxyl-Stretching Wavenumbers and Composition of Micas in the System K<sub>2</sub>O-MgO-Al<sub>2</sub>O<sub>3</sub>-SiO<sub>2</sub>-H<sub>2</sub>O: A Single Model for Trioctahedral and Dioctahedral Micas. *Am. J. Sci.*, **1988**, 288-A, 199-212.
- (4). B. Smith, ed., Infrared Spectral Interpretation: a Systematic Approach, CRC Press, **1999**.
- (5) Sposito, G. and Prost, R., Structure of Water Adsorbed on Smectites. *Chem. Rev.*, **1982**, 82, 553-573.
- (6) Xu, W., Johnston, C.T., Parker, P. and Agnew, S.F., Infrared Study of Water Sorption on Na-, Li-, Ca-, and Mg-Exchanged (SWy-1 and SAz-1) Montmorillonite. *Clays Clay Miner.*, **2000**, 48, 120-131.

## SI-2: Thermogravimetric Analysis (TGA) of talc

Thermogravimetric Analysis (TGA) measurements are performed with a Mettler-Toledo TGA/DSC 1 analyzer. The samples (approximately 20 mg) are placed in an alumina crucible of 70  $\mu\text{L}$  and heated from 25 to 900  $^{\circ}\text{C}$  at a heat flow of 10  $^{\circ}\text{C}.\text{min}^{-1}$  under a dinitrogen flux of 50  $\text{mL min}^{-1}$  and then cooled to room temperature. The data are analyzed using the STAR<sup>e</sup> software.

Figure S2 evidences that water is not detected. The ATG curve is modified neither by the relative humidity (not shown here) nor by irradiation. The same results are obtained for both synthetic and natural talc. This is consistent with the non-swelling character of talc.

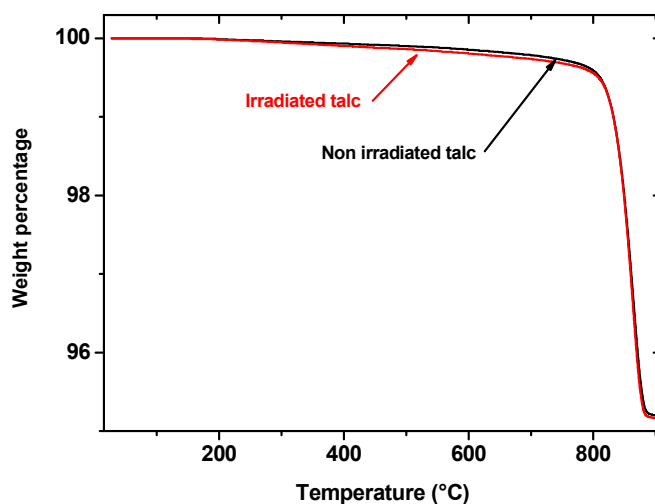


**Figure S2.** TGA analysis for synthetic talc equilibrated at a 3% relative humidity. No dehydration feature (around 100°C) is observed indicating that the water weight percentage remains equal to 0 %.

### SI-3: X-Ray Diffraction (XRD) of talc

Powder X-ray patterns are collected on a Bruker D8 Advance diffractometer. The X-ray diffraction setup is equipped with a grazing parabolic Göbel mirror and a Cu emitter ( $\lambda_{\text{CuK}\alpha} = 1.541 \text{ \AA}$ , 40 kV/40 mA). The diffracted beam is collected by a Vantek detector which is a position sensitive detector. The  $d_{001}$  value obtained for both talcs is  $9.43 \pm 0.02 \text{ \AA}$  which proves that there is no water layer in the interlayer space.<sup>1-5</sup>

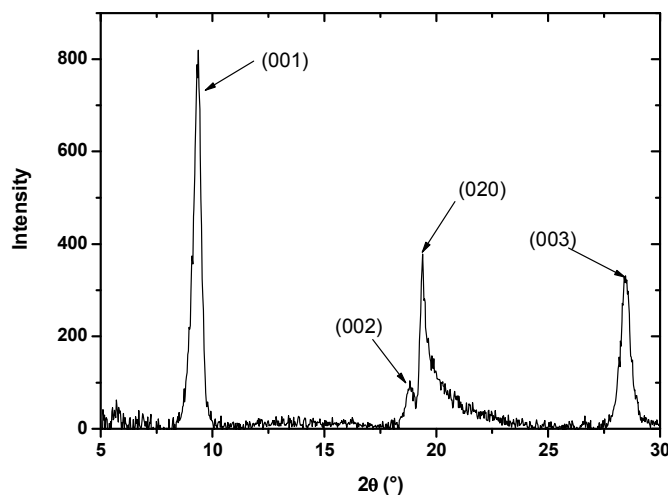


**Figure S3.** XRD pattern of the synthetic talc sample.

The diffraction patterns of both talc samples are given in Figure S4. The relative intensities of the (001)/(002)/(003) reflections are the same for the natural and synthetic talc. The widths of the reflections for the synthetic sample are larger than for the natural sample, which corresponds to smaller Coherent Diffraction Domains (CDD) and which is also in line with smaller particles observed by SEM for synthetic talc as compared to natural talc. There is also a preferred mean particle orientation, as the (020) reflection has the same intensity for both talc samples contrary to the other reflections which are higher for natural talc than for the synthetic sample.

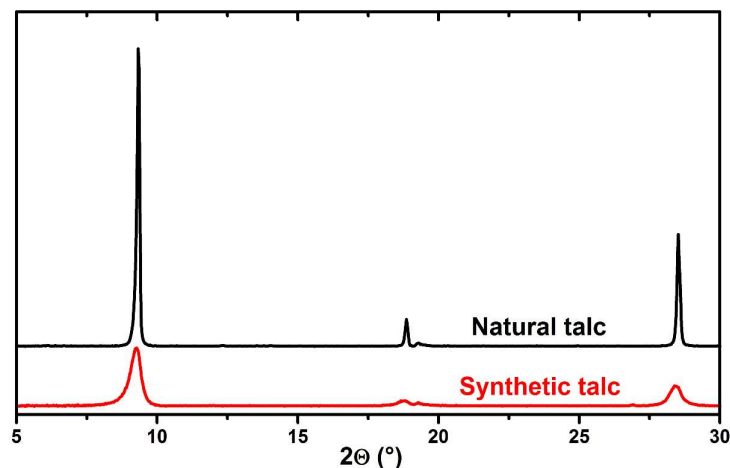


**Figure S4.** Diffraction diagrams of synthetic (–) and natural talc (–). Both diagrams were recorded under the same experimental conditions.

## References:

- (1) Bradley, W.F., Grim, R.E., and Clark, G.F., A Study of the Behavior of Montmorillonite on Wetting. *Z. Kristallogr.*, **1937**, 97, 216-222.
- (2). Dumas, A., Martin, F., Ferrage, E., Micoud, P., Le Roux, C. and Petit, S., Synthetic Talc Advances: Coming Closer to Nature, Added Value, and Industrial Requirements. *Appl. Clay Sci.*, **2013**, 85, 8-18.
- (3) Mooney, R.W., Keenan, A.G. and Wood, L.A., Adsorption of Water Vapor by Montmorillonite. II. Effect of Exchangeable Ions and Lattice Swelling as Measured by X-Ray Diffraction. *J. Am. Chem. Soc.*, **1952**, 74, 1371-1374.
- (4) Nagelschmidt, G., On the Lattice Shrinkage and Structure of Montmorillonite. *Z. Kristallogr.*, **1936**, 93, 481-487.
- (5) Norrish, K., The Swelling of Montmorillonite. *Disc. Faraday Soc.*, **1954**, 18, 120-134.

**SI-4: H<sub>2</sub> Radiolytic yield (G<sub>H<sub>2</sub></sub>) of irradiated talc as a function of the relative humidity**

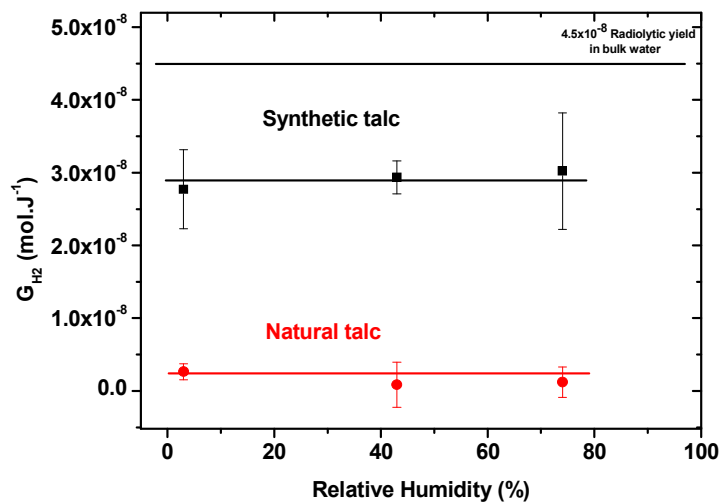


**Figure S5.** H<sub>2</sub> radiolytic yields as a function of the relative humidity for synthetic and natural talc. The value obtained in bulk water is given as a reference (4.5 x 10<sup>-8</sup> mol.J<sup>-1</sup>). The H<sub>2</sub> radiolytic yield does not depend on the relative humidity.

**SI-5: Evolution of the EPR signal as a function of the dose for synthetic talc (at 298 K)**

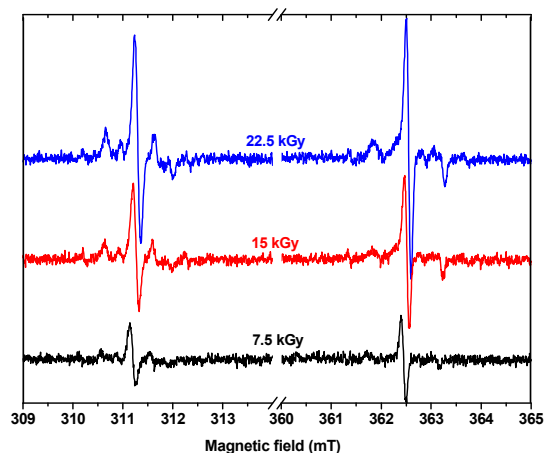


**Figure S6.** EPR Spectrum of  $H^\bullet$  radical in synthetic talc irradiated at different doses: black line 7.5 kGy, red line 15 kGy and blue line 22.5 kGy.

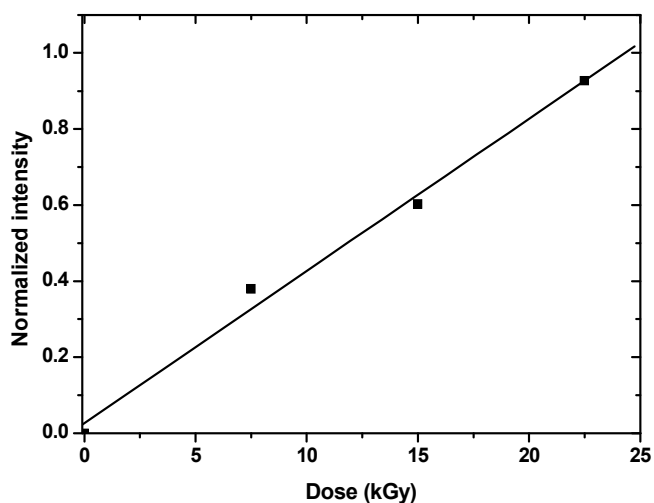


**Figure S7.** Evolution of the normalized intensity (according to the weight of each sample) of the  $H^\bullet$  signal in synthetic talc as a function of the dose and the corresponding linear fit. The slope of the line is  $(4.0 \pm 0.4) \times 10^{-5} \text{ Gy}^{-1}$ .



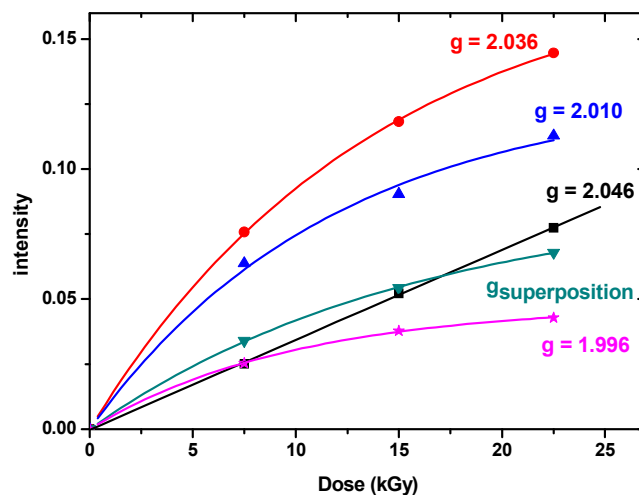


**Figure S8.** Evolution of the intensity (normalized with respect to the weight and volume of the sample) of each EPR defect as function of the dose and the corresponding fit ( $y=a*x$  or  $y=c*(1-\exp(-d*x))$ ): black squares (■) corresponds to  $g = 2.046$ , red dots (●) to  $g = 2.036$ , blue triangle (▲) to  $g = 2.010$ , dark cyan reverse triangle (▼)  $g_{\text{superposition}}$  and purple stars (★) to  $g = 1.996$ . The fit parameters are the following: for  $g = 2.046$ ,  $a = 0.00259$ ; for  $g = 2.036$ ,  $c = 0.179$  and  $d = 0.072$ ; for  $g = 2.010$ ,  $c = 0.130$  and  $d = 0.08$ ; for  $g_{\text{superposition}}$ ,  $c = 0.089$  and  $d = 0.063$ ; and for  $g = 1.996$ ,  $c = 0.048$  and  $d = 0.0101$ .

The amount of trapped  $H^\bullet$  atoms in the talc structure is linear with the dose in the dose range studied (1-25 kGy) (Figure S7). It is not the case for the other defects (Figure S8). Therefore, we chose the 15 kGy dose for the EPR experiments.

## SI-6: Evolution of the EPR signal as a function of the microwave power for synthetic talc

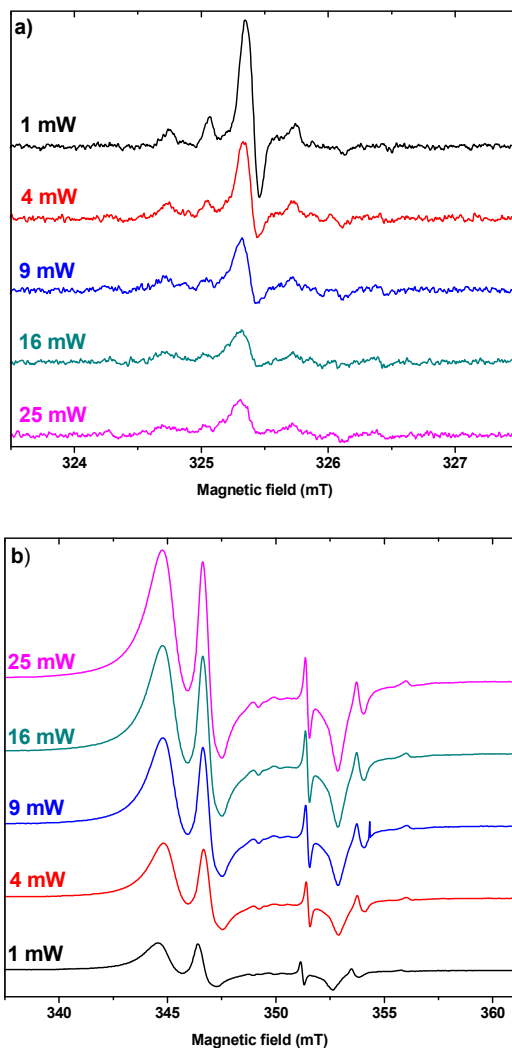


**Figure S9.** EPR spectra of synthetic talc irradiated at 15 kGy and recorded at 298 K as a function of the microwave power for a) the left side component of the  $H^\bullet$  signal and b) the defects signal.

The  $H^\bullet$  signal and the defects signal present an opposite behavior with the microwave power: the defects signal increases with the microwave power whereas the  $H^\bullet$  signal decreases. There is no difference between the different parts of defects signal, making this microwave study useless for the defects identification. All EPR experiments were thus performed with a microwave power of 1 mW for which the  $H^\bullet$  signal is the strongest and the defects signal is strong enough to be analyzed.

Therefore, the choice of the 15 kGy dose and of the 1 mW microwave power was found to be a good compromise for the EPR measurements.